

**Energy transport between heat baths with oscillating temperatures**Renai Chen<sup>1</sup>, Tammie Gibson<sup>2</sup>, and Galen T. Craven<sup>2</sup><sup>1</sup>Theoretical Division and Center for Nonlinear Studies, Los Alamos National Laboratory, Los Alamos, New Mexico 87545, USA<sup>2</sup>Theoretical Division, Los Alamos National Laboratory, Los Alamos, New Mexico 87545, USA

(Received 6 April 2023; accepted 11 July 2023; published 31 August 2023)

Energy transport is a fundamental physical process that plays a prominent role in the function and performance of myriad systems and technologies. Recent experimental measurements have shown that subjecting a macroscale system to a time-periodic temperature gradient can increase thermal conductivity in comparison to a static temperature gradient. Here, we theoretically examine this mechanism in a nanoscale model by applying a stochastic Langevin framework to describe the energy transport properties of a particle connecting two heat baths with different temperatures, where the temperature difference between baths is oscillating in time. Analytical expressions for the energy flux of each heat bath and for the system itself are derived for the case of a free particle and a particle in a harmonic potential. We find that dynamical effects in the energy flux induced by temperature oscillations give rise to complex energy transport hysteresis effects. The presented results suggest that applying time-periodic temperature modulations is a potential route to control energy storage and release in molecular devices and nanosystems.

DOI: [10.1103/PhysRevE.108.024148](https://doi.org/10.1103/PhysRevE.108.024148)**I. INTRODUCTION**

Discovering and understanding the fundamental physical mechanisms governing energy transport processes at the nanoscale is one of the most important problems in the molecular sciences [1–10]. Vibrational, electronic, and radiative energy transport mechanisms, as well as their interplay, manifest at the nanoscale in complex nonequilibrium processes [7,11–29]. Gaining a deeper understanding of these mechanisms is becoming increasingly important to advance the development of multiple technologies. Energy transport plays a prominent role in the function of physical, biological, and technological systems [4,11,30]. Therefore, developing accurate theoretical tools to describe energy transport processes is critical. At the nanoscale, controlling energy transport in the form thermal energy, i.e., heat, has broad applications to advance the design of electronic devices [2,31–33], thermoelectric molecules and materials [34–37], and phononic systems that use heat to perform logical operations [11,21,38]. Recent advances in the ability to probe energy transport at the atomistic level, both theoretically [39,40] and experimentally [41,42], facilitate the use and manipulation of energy transport properties in practical molecular applications.

There have been significant recent advances in the experimental set-ups used to examine nanoscale heat transport. Specifically, several groups have developed experimental techniques capable of measuring thermal conductance at the single-molecule level [41,42]. These advances open the pos-

sibility to probe, characterize, and utilize energy transport effects by tailoring molecular structural characteristics. Energy transport through molecular structures typically involves complex nonequilibrium dynamics [18,38,43–46] due to the interplay between multiple heat transport mechanisms at the nanoscale. Advanced theoretical tools are therefore needed to describe these nanoscale processes, which typically do not follow macroscale principles, for example, Fourier’s law [47–51].

At the macroscale, periodic modulation of a temperature gradient can enhance heat flow leading to increased thermal conductivity in comparison to a static temperature gradient [52]. However, the molecular origins of this enhanced thermal conductivity have not been established. Here, we explore how the thermal transport properties of a model nanoscale system can be modified by applying periodic temperature modulations. Time-dependent temperatures can be used to affect, control, and probe molecular properties of systems ranging in size from large macromolecules to single atoms [53–55]. Temperature modulations play a prominent role in the function of a multitude of systems including: pyroelectric materials [56–58], thermal batteries [59,60], molecular ratchets [61–63], thermal devices with memory [64,65], and calorimetry devices [66,67].

In this article, we use a paradigmatic model of a nanoscale system to examine the energy transport properties of a particle connecting two heat baths with different temperatures, where the temperature difference between baths is periodic in time (see Fig. 1). Theoretical frameworks describing the thermodynamics of a system in contact with one or more heat baths with time-dependent temperatures have a rich history [68–78]. However, these previously developed theoretical formalisms cannot be used to accurately describe the model we consider in this article because of one or more of the following:

Published by the American Physical Society under the terms of the [Creative Commons Attribution 4.0 International](https://creativecommons.org/licenses/by/4.0/) license. Further distribution of this work must maintain attribution to the author(s) and the published article’s title, journal citation, and DOI.

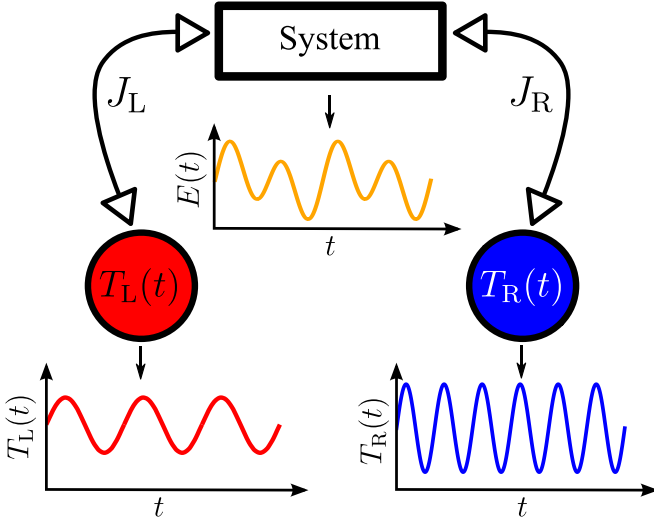


FIG. 1. Schematic diagram of the model used in this work. The system, represented by a labeled rectangle, is in contact with two heat baths, L(left) and R(right). Bath L is represented by a red circle and bath R is represented by a blue circle. The time-dependent temperatures of the baths are  $T_L(t)$  and  $T_R(t)$ . The temperatures of each bath are oscillating in time, as illustrated by the graphs at the bottom of the figure. The energy of the system  $E(t)$  oscillates due to the temperature oscillations. The black curves with arrows illustrate the energy flow channels in the model. The energy fluxes in/out of each bath are  $J_L$  and  $J_R$ .

(a) they are constructed for the case of a system in contact with a single heat bath and therefore do not describe energy transport properties between multiple baths with different temperatures, (b) they are derived from macroscale principles that do not accurately capture nanoscale energy transport properties, and/or (c) they assume the system is in a quasistatic state and therefore do not describe the limit of fast temperature oscillations.

The specific theoretical formalism we apply is a stochastic Langevin equation describing a single particle that bridges two heat baths with oscillating temperatures. The time-dependent temperature difference between the two baths affects the energy transport through the system (the particle) and results in phenomena, for example, energy flux hysteresis, that are not present in the case of a static temperature difference. Analytical expressions for the different energy fluxes in the model, specifically the energy flux from each bath and from particle itself, are derived for the case of a free particle and a particle in a harmonic potential. The results of stochastic molecular dynamics simulations are in strong agreement with the derived results, supporting the validity of the derived energy flux expressions. We find that the energy transport properties can be significantly altered by the temperature oscillations.

The remainder of the article is organized as follows: Section II contains a description of the model used to examine energy transport between heat baths with oscillating temperatures. In Sec. III, the definitions and general formalism for energy transport are presented, including definitions of how the energy fluxes in the model are determined. Section IV contains derivations of the energy flux expressions for two cases:

(a) a free particle (Sec. IV A) and (b) a particle in a harmonic potential (Sec. IV B). Results and discussion about each case are included in the corresponding section. Conclusions and future directions are presented in Sec. V.

## II. MODEL

The model we use to examine nanoscale heat transport in the presence of temperature oscillations consists of a single particle that is in contact with two heat baths, both of which have temperatures that are oscillating in time. Specifically, the two heat baths, denoted by L for “left” bath and R for “right” bath, have periodically oscillating temperatures  $T_L(t) = T_L(t + \mathcal{T}_L)$  and  $T_R(t) = T_R(t + \mathcal{T}_R)$  where  $\mathcal{T}_L$  and  $\mathcal{T}_R$  are the respective periods of oscillation. A schematic diagram of the model is shown in Fig. 1. The Langevin equation of motion for the system is

$$\begin{aligned} \dot{x} &= v, \\ \dot{v} &= -\gamma_L \dot{x} - \gamma_R \dot{x} - m^{-1} \partial_x U(x) + \xi_L(t) + \xi_R(t), \end{aligned} \quad (1)$$

where  $x$  is the position of the particle,  $v$  is the particle velocity,  $U(x)$  is the potential energy,  $\gamma_L$  and  $\gamma_R$  are dissipative (friction) terms for each bath that parametrize the system-bath coupling strength, and  $\xi_L(t)$  and  $\xi_R(t)$  are stochastic noise terms that obey the following correlations:

$$\begin{aligned} \langle \xi_L(t) \xi_L(t') \rangle &= 2\gamma_L k_B m^{-1} T_L(t) \delta(t - t'), \\ \langle \xi_R(t) \xi_R(t') \rangle &= 2\gamma_R k_B m^{-1} T_R(t) \delta(t - t'), \\ \langle \xi_L(t) \xi_R(t') \rangle &= 0, \\ \langle \xi_L(t) \rangle &= 0, \\ \langle \xi_R(t) \rangle &= 0, \end{aligned} \quad (2)$$

where  $m$  is the particle mass and  $k_B$  is the Boltzmann constant. The notation  $\langle \dots \rangle$  denotes an average over realizations of the noise. These correlations are at the Markovian limits describing the physical situation in which the intensity (strength) of the noise of each bath is oscillating in time, and that intensity depends on the temperature of that bath at the current time  $t$  but not on the temperature at previous times  $t'$ . Theoretical formulations of time-dependent temperatures that include non-Markovian effects have been developed [70,71]. Here we will only examine the Markovian case. Specifically, Eq. (1) is a special two-bath memoryless limit of the generalized Langevin equation derived in Ref. [70]. We will examine two cases for the potential: a free particle with  $U(x) = 0$  and a particle in a harmonic potential  $U(x) = \frac{1}{2} m k x^2$ . We define the temperatures of each bath to take the specific oscillatory forms

$$T_L(t) = T_L^{(0)} + \Delta T_L \sin(\omega_L t), \quad (3)$$

$$T_R(t) = T_R^{(0)} + \Delta T_R \sin(\omega_R t), \quad (4)$$

where  $T_L^{(0)}$  and  $T_R^{(0)}$  are the temperatures of the two baths in the limit of vanishing of oscillations,  $\Delta T_L$  and  $\Delta T_R$  define the amplitude of the oscillations, and  $\omega_L$  and  $\omega_R$  are oscillation

frequencies. In the case in which  $\omega_L$  and  $\omega_R$  are commensurable, the system and heat currents are periodic, and we denote the total period of the model as  $\mathcal{T}$ . The instantaneous temperature difference between the two baths is

$$\Delta T(t) = T_L(t) - T_R(t). \quad (5)$$

### III. HEAT TRANSPORT

The energetic properties of the system can be described using the Sekimoto formalism for stochastic energetics [79] which involves separating the terms in Eq. (1) into contributions to the system energy change and contributions to the energy change in the baths. We specifically separate the expected energy fluxes in our model into three terms:

(1)  $J_{\text{sys}}$  is the energy flux in/out of the system. It is generated by changes in the energy of the system. Part of the energy transferred by this flux will be partitioned to the right bath and part will be partitioned to the left bath.

(2)  $J_L$  is the energy flux associated with the left bath.

(3)  $J_R$  is the energy flux associated with the right bath.

The sum of the energy fluxes obeys conservation of energy:  $J_L(t) + J_R(t) + J_{\text{sys}}(t) = 0$ . Using the stochastic energetics formalism, the expected energy fluxes in/out of the baths and the system (see Fig. 1) can be expressed as [12,13,20,79]

$$J_L(t) = m\gamma_L \langle v^2(t) \rangle - m \langle \xi_L(t)v(t) \rangle, \quad (6)$$

$$J_R(t) = m\gamma_R \langle v^2(t) \rangle - m \langle \xi_R(t)v(t) \rangle, \quad (7)$$

$$J_{\text{sys}}(t) = \partial_t \langle E(t) \rangle, \quad (8)$$

where  $E(t)$  is the energy of the system,  $\langle v^2(t) \rangle$  is the second velocity moment of the system, and  $\langle \xi_L(t)v(t) \rangle$  and  $\langle \xi_R(t)v(t) \rangle$  are noise-velocity correlation functions. We use a sign convention such that the energy flux expressions are positive when energy enters the corresponding bath/system and negative when energy leaves the bath/system. The system energy flux can be separated into the sum of two parts

$$J_{\text{sys}}(t) = J_{\text{sys}}^{(L)}(t) + J_{\text{sys}}^{(R)}(t), \quad (9)$$

where  $J_{\text{sys}}^{(L)}$  and  $J_{\text{sys}}^{(R)}$  are the part of the system energy flux that flows in/out of the left bath and right bath, respectively.

Because the bath temperatures are varying, the system will not reach a nonequilibrium steady state (NESS). Instead, the system approaches a time-dependent nonequilibrium state (TDNS) with an average energy that is oscillating in time. In a system that is in a NESS,  $\partial_t \langle E(t) \rangle = 0$  and  $J_L(t) = -J_R(t)$ . However, in the case of periodic temperatures the system energy can be a time-dependent quantity leading to a nonvanishing derivative of the energy with respect to time.

Our analysis will focus on examining the heat current properties over a period of oscillation. The expected heat that is obtained/released by the baths or the system  $K \in \{L, R, \text{sys}\}$  over the time interval  $[0, \mathcal{T}]$  is

$$\mathcal{Q}_K = \int_0^{\mathcal{T}} J_K(t') dt'. \quad (10)$$

For the purpose of examining energy storage capabilities of the system, it will often be useful to separate the total energy change  $\mathcal{Q}_K$  into two parts [80], the energy obtained by the

bath/system

$$\mathcal{Q}_K^+ = \int_0^{\mathcal{T}} J_K(t') \Theta[J_K(t')] dt', \quad (11)$$

and the energy lost by the bath/system

$$\mathcal{Q}_K^- = \int_0^{\mathcal{T}} J_K(t') \Theta[-J_K(t')] dt', \quad (12)$$

where  $\Theta$  is the Heaviside function.

## IV. ENERGY FLUX DERIVATION AND RESULTS

### A. Free particle

We first examine the case of free particle by setting  $U(x) = 0$ . The equation of motion for a free particle connected to two thermal baths can be expressed as

$$\begin{aligned} \dot{x} &= v, \\ \dot{v} &= -\gamma \dot{x} + \xi_L(t) + \xi_R(t), \end{aligned} \quad (13)$$

with

$$\gamma = \gamma_L + \gamma_R, \quad (14)$$

being the effective friction. It is important to note that in our analysis we will not assume that the system is in a quasistatic nonequilibrium state. Because we do not make the quasistatic assumptions, inertial effects due to the oscillating temperatures can significantly affect the system's heat transport properties.

The equation of motion (13) is solved by the set of equations:

$$\begin{aligned} x(t) &= x_0 + \int_0^t v(s) ds, \\ v(t) &= v_0 e^{-\gamma t} + \int_0^t e^{-\gamma(t-s)} \xi_L(s) ds + \int_0^t e^{-\gamma(t-s)} \xi_R(s) ds, \end{aligned} \quad (15)$$

where  $x_0$  is the initial position and  $v_0$  is the initial velocity of the particle. These formal solutions can be applied to construct expressions for the moments and time-correlation functions of a particle driven by two thermal sources. The average energy of the system, that is of the particle, is

$$\langle E(t) \rangle = \frac{1}{2} m \langle v^2(t) \rangle. \quad (16)$$

Note that in the *absence* of temperature oscillations, i.e., in the  $(\Delta T_L, \Delta T_R) \rightarrow (0, 0)$  limit, the system reaches a nonequilibrium steady state in which the energy of the system is [70,79,81–83]

$$\langle E \rangle = \frac{1}{2} k_B T, \quad (17)$$

where

$$T = \frac{\gamma_L T_L^{(0)} + \gamma_R T_R^{(0)}}{\gamma_L + \gamma_R} \quad (18)$$

is the effective temperature of the system.

To evaluate the energy flux for a free particle, we will need to evaluate the correlation functions in Eqs. (6)–(8). The noise-velocity correlation functions  $\langle \xi_L(t)v(t) \rangle$  and  $\langle \xi_R(t)v(t) \rangle$  for a free particle can be constructed using Eq. (15),

$$\langle \xi_L(t)v(t) \rangle = \langle \xi_L(t)v_0 \rangle e^{-\gamma t} + \int_0^t e^{-\gamma(t-s)} \langle \xi_L(t)\xi_L(s) \rangle ds + \int_0^t e^{-\gamma(t-s)} \langle \xi_L(t)\xi_R(s) \rangle ds = \frac{\gamma_L k_B T_L(t)}{m}, \quad (19)$$

$$\langle \xi_R(t)v(t) \rangle = \langle \xi_R(t)v_0 \rangle e^{-\gamma t} + \int_0^t e^{-\gamma(t-s)} \langle \xi_R(t)\xi_L(s) \rangle ds + \int_0^t e^{-\gamma(t-s)} \langle \xi_R(t)\xi_R(s) \rangle ds = \frac{\gamma_R k_B T_R(t)}{m}, \quad (20)$$

where we have utilized  $\langle \xi_L(t)v_0 \rangle = \langle \xi_R(t)v_0 \rangle = 0$  and the correlations in Eq. (2) to complete the evaluation.

The other correlation function that must be evaluated to obtain analytical expressions for the energy fluxes is  $\langle v^2(t) \rangle$ . Squaring the formal solution in Eq. (15) and applying the correlations in Eq. (2) yields

$$\begin{aligned} \langle v^2(t) \rangle &= v_0^2 e^{-2\gamma t} + \int_0^t \int_0^t e^{-\gamma(2t-s_1-s_2)} \langle \xi_L(s_1)\xi_L(s_2) \rangle ds_1 ds_2 + \int_0^t \int_0^t e^{-\gamma(2t-s_1-s_2)} \langle \xi_R(s_1)\xi_R(s_2) \rangle ds_1 ds_2 \\ &+ 2 \int_0^t e^{-\gamma(2t-s_1)} \langle \xi_L(s_1)v_0 \rangle ds_1 + 2 \int_0^t e^{-\gamma(2t-s_1)} \langle \xi_R(s_1)v_0 \rangle ds_1 + 2 \int_0^t \int_0^t e^{-\gamma(2t-s_1-s_2)} \langle \xi_L(s_1)\xi_R(s_2) \rangle ds_1 ds_2, \\ &= v_0^2 e^{-2\gamma t} + \frac{k_B T}{m} (1 - e^{-2\gamma t}) \\ &+ \frac{2k_B}{m} \left( \frac{\gamma_L \Delta T_L (2\gamma \sin(\omega_L t) - \omega_L \cos(\omega_L t) + \omega_L e^{-2\gamma t})}{4\gamma^2 + \omega_L^2} + \frac{\gamma_R \Delta T_R (2\gamma \sin(\omega_R t) - \omega_R \cos(\omega_R t) + \omega_R e^{-2\gamma t})}{4\gamma^2 + \omega_R^2} \right). \quad (21) \end{aligned}$$

The last three terms in the top equation vanish because  $\langle \xi_L(t)v_0 \rangle = 0$ ,  $\langle \xi_R(t)v_0 \rangle = 0$ , and  $\langle \xi_L(t)\xi_R(t') \rangle = 0$ . In the limit of vanishing temperature oscillations,  $\langle v^2(t) \rangle = v_0^2 e^{-2\gamma t} + k_B T/m(1 - e^{-2\gamma t})$ , where the effective temperature  $T$  is defined in Eq. (18). In the long-time limit this expression reduces to  $\langle v^2(t) \rangle = k_B T/m$ .

A fraction of the total energy flux is energy that is obtained/released by the particle, the rest being heat current between baths. In the long time limit, the system approaches a time-dependent (oscillatory) nonequilibrium state. In this limit, the exponential terms vanish and the energy flux expressions simplify to

$$J_L(t) = \gamma_L k_B \left( T - T_L(t) + \frac{2\gamma_L \Delta T_L [2\gamma \sin(\omega_L t) - \omega_L \cos(\omega_L t)]}{4\gamma^2 + \omega_L^2} + \frac{2\gamma_R \Delta T_R [2\gamma \sin(\omega_R t) - \omega_R \cos(\omega_R t)]}{4\gamma^2 + \omega_R^2} \right), \quad (22)$$

$$J_R(t) = \gamma_R k_B \left( T - T_R(t) + \frac{2\gamma_L \Delta T_L [2\gamma \sin(\omega_L t) - \omega_L \cos(\omega_L t)]}{4\gamma^2 + \omega_L^2} + \frac{2\gamma_R \Delta T_R [2\gamma \sin(\omega_R t) - \omega_R \cos(\omega_R t)]}{4\gamma^2 + \omega_R^2} \right), \quad (23)$$

$$J_{\text{sys}}(t) = k_B \left( \frac{\gamma_L \Delta T_L \omega_L [2\gamma \cos(\omega_L t) + \omega_L \sin(\omega_L t)]}{4\gamma^2 + \omega_L^2} + \frac{\gamma_R \Delta T_R \omega_R [2\gamma \cos(\omega_R t) + \omega_R \sin(\omega_R t)]}{4\gamma^2 + \omega_R^2} \right), \quad (24)$$

which are independent of the initial velocity  $v_0$ . Equations (22)–(24) are the primary results of this subsection. They are analytical expressions for the energy fluxes generated in the TDNS. It is also important to note that because the system is in a TDNS, the net energy flux from the system  $J_{\text{sys}}(t)$  does not vanish. It can be verified that by combining Eqs. (22)–(24), the conservation of energy relation

$$J_L(t) + J_R(t) + J_{\text{sys}}(t) = 0 \quad (25)$$

is satisfied.

In the limit of quasistatic (QS) temperature oscillations, at every time instant the system is characterized by a Gibbs distribution with effective temperature

$$T^{(\text{QS})}(t) = \frac{\gamma_L T_L(t) + \gamma_R T_R(t)}{\gamma_L + \gamma_R}. \quad (26)$$

The QS limit implies that the temperature of the bath is varying slowly enough such that the relaxation rate of the system  $\gamma$  is much faster than the oscillation rates of both temperatures. In the QS limit defined by  $(\omega_L/\gamma, \omega_R/\gamma) \rightarrow (0, 0)$ , the energy

flux expressions reduce to

$$\begin{aligned} J_L^{(\text{QS})}(t) &= k_B \frac{\gamma_L \gamma_R}{\gamma_L + \gamma_R} [T_R(t) - T_L(t)], \\ J_R^{(\text{QS})}(t) &= k_B \frac{\gamma_L \gamma_R}{\gamma_L + \gamma_R} [T_L(t) - T_R(t)], \quad (27) \end{aligned}$$

$$J_{\text{sys}}^{(\text{QS})}(t) = 0.$$

In the limit of vanishing temperature oscillations  $(\Delta T_L, \Delta T_R) \rightarrow (0, 0)$ , which we will refer to as the static (S) limit, the energy flux expressions reduce to the forms

$$\begin{aligned} J_L^{(\text{S})} &= k_B \frac{\gamma_L \gamma_R}{\gamma_L + \gamma_R} (T_R^{(0)} - T_L^{(0)}), \\ J_R^{(\text{S})} &= k_B \frac{\gamma_L \gamma_R}{\gamma_L + \gamma_R} (T_L^{(0)} - T_R^{(0)}), \quad (28) \\ J_{\text{sys}}^{(\text{S})} &= 0, \end{aligned}$$

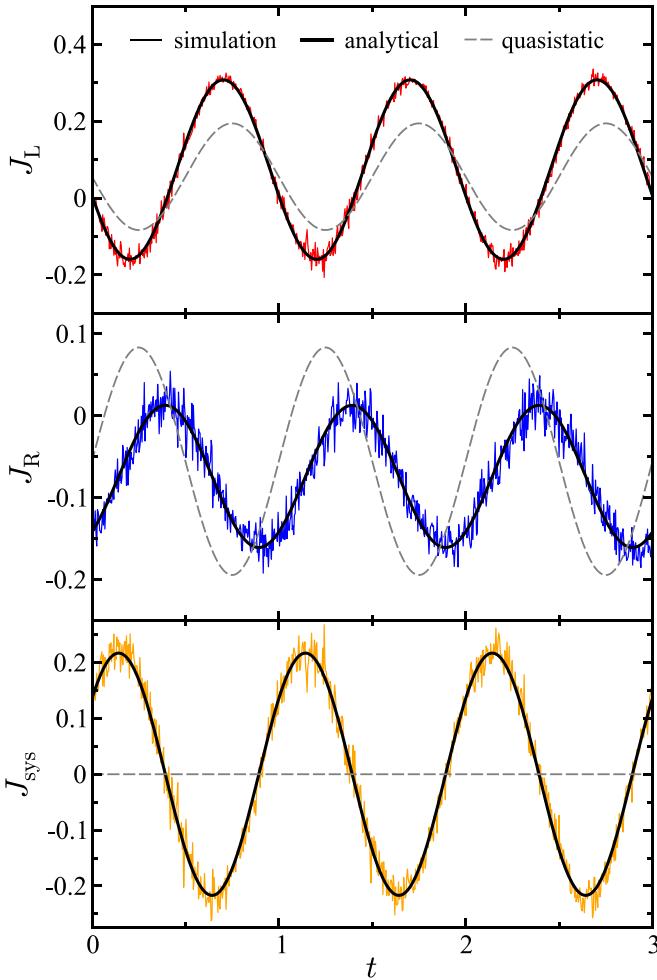


FIG. 2. Time-dependence of the energy fluxes for the left bath (top), right bath (middle), and the system (bottom) in the case of a free particle connecting two heat baths with oscillating temperatures. Each energy flux is shown in units of  $\gamma k_B T$ . Time is shown in units of the total oscillation period  $\mathcal{T}$ . Parameters are  $\gamma = 2$  ( $\gamma_L = 1, \gamma_R = 1$ ),  $m = 1$ ,  $T_L^{(0)} = 0.8$ ,  $T_R^{(0)} = 1.07$ ,  $\Delta T_L = 0.5$ ,  $\Delta T_R = 0$ ,  $\omega_L = 5$ ,  $\omega_R = 0$ . All parameters throughout are given in reduced units with characteristic dimensions:  $\tilde{\sigma} = 1 \text{ \AA}$ ,  $\tilde{\tau} = 1 \text{ ps}$ ,  $\tilde{m} = 10 m_u$ , and  $\tilde{T} = 300 \text{ K}$ . In each panel, the black curve is the exact analytical result, the dashed gray curve is the result given by the corresponding quasistatic expression, and the noisy colored curves are the results generated from molecular dynamics simulations.

which do not depend on time. These are well-known forms for the heat current of a single particle in contact with two heat baths with different temperatures [13].

Shown in Fig. 2 are the energy fluxes of the left bath, the right bath, and the system for the situation in which the temperature of one bath is oscillating and the temperature of the other bath is constant. Both the analytical results and the results of molecular dynamics (MD) simulations are shown. The MD results are generated by integrating Eq. (1) using the Euler-Maruyama scheme and then calculating the energy fluxes using the stochastic energetics formalism [12,79]. The parameters for all simulations in this article are given in reduced units with characteristic dimensions:  $\tilde{\sigma} = 1 \text{ \AA}$ ,  $\tilde{\tau} = 1 \text{ ps}$ ,  $\tilde{m} = 10 m_u$ , and  $\tilde{T} = 300 \text{ K}$ . The parameter values used

in all figures are listed in Table I in the Appendix. The results of the MD simulations are in excellent agreement with the analytical results for all three energy fluxes in the model. It can be observed that even though the temperature of the right bath is not oscillating, the effect of the oscillating left bath temperature propagates through the system, causing periodic fluctuations in the energy flux of the right bath. In the quasistatic limit, the energy fluxes of the left and right baths have the same magnitude but opposite signs while the system energy flux is zero at all times. Significant differences in the energy flux oscillation phase and magnitude are observed between the exact analytical result and the quasistatic result. These effects will play an important role in the generation of the energy flux hysteresis, which is discussed later.

The energy fluxes for the case in which the temperatures of both baths are oscillating at different frequencies are shown in Fig. 3. The system-bath couplings are asymmetric, with the coupling being stronger for the left bath than for the right bath,  $\gamma_L > \gamma_R$ . In this case, complex dynamics are observed. The oscillation frequency of the strongly coupled left bath is dominant in the energy flux of the left bath while the weakly coupled right bath exhibits features of multiple frequencies, meaning it is influenced by the oscillations of both baths. The system energy flux exhibits a complex pattern, combining the functional characteristics of the left bath and right bath energy fluxes. This is because all the energy that is transported from the left bath to right bath goes through the system, hence the system takes on characteristics of both bath energy fluxes. In the quasistatic limit, the left and right fluxes are a mix of the two sinusoidal temperature oscillation patterns, and, interestingly, are more aligned with the weakly coupled right bath oscillation pattern. The system energy flux vanishes in the quasistatic limit. The MD results are in excellent agreement with the analytical results over all these complex trends.

Hysteresis effects in electronic fluxes are of significant interest in the field of neuromorphic computing and, more broadly, in the development of logical devices with memory [84–87]. Dynamical effects in the energy fluxes induced by fast temperature oscillations relative to the system relaxation rate (the system-bath coupling) can generate hysteresis effects. We will refer to these effects as inertial effects. Using the derived energy flux expressions, we find that in the limit of fast temperature oscillations in comparison to the system relaxation timescale  $\gamma$ , the energy transport properties can be significantly different than in the quasistatic limit of slow temperature oscillations. In Fig. 4, the energy fluxes in the model are shown as a function of the time-dependent temperature difference between baths  $\Delta T(t)$ . The  $t = 0$  starting point in each hysteresis loop is denoted by a circular marker. Using the exact analytical results, hysteresis is observed in all of the energy fluxes, meaning that the same temperature difference can generate different flux values depending on the time in the temperature oscillation period. This differs from the quasistatic limit where the hysteresis effects vanish, as shown by the solid black lines. We also observe transient energy transport in the direction that goes against the thermal gradient, that is, time periods in the oscillation cycle where heat flows in the cold to hot direction. However, this effect is only transient, and the net heat flow, i.e., the average energy flux, is always in the direction (hot to cold) that obeys ther-

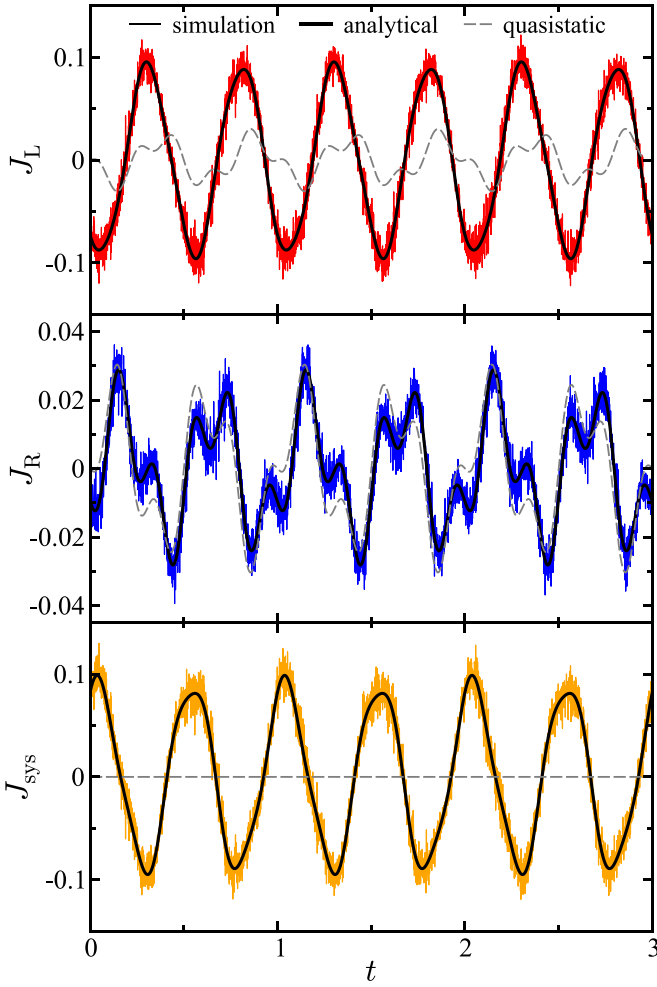


FIG. 3. Time-dependence of the energy fluxes for the left bath (top), right bath (middle), and the system (bottom) in the case of a free particle connecting two heat baths with oscillating temperatures. Each energy flux is shown in units of  $\gamma k_B T$ . Time is shown in units of the total oscillation period  $\mathcal{T}$ . Parameters are  $\gamma = 1.7$  ( $\gamma_L = 1.5$ ,  $\gamma_R = 0.2$ ),  $m = 1$ ,  $T_L^{(0)} = 1$ ,  $T_R^{(0)} = 1$ ,  $\Delta T_L = 0.2$ ,  $\Delta T_R = 0.1$ ,  $\omega_L = 2$ ,  $\omega_R = 5$ . In each panel, the black curve is the exact analytical result, the dashed gray curve is the result given by the corresponding quasistatic expression, and the noisy colored curves are the results generated from molecular dynamics simulations.

modynamics principles. The quasistatic results are shown as black lines in each panel. In this limit, no hysteresis effects are observed.

Energy flux hysteresis loops are shown in Fig. 5 for the case in which the temperatures of both baths are oscillating, but at different frequencies. Because of inertial effects brought on by fast temperature oscillations, the energy fluxes are not zero when  $\Delta T = 0$ . The patterns generated are reminiscent of Lissajous curves, but the interweaving paths and asymmetric shapes result in complex loops and should be attributed to the complexities that arise from fast temperature oscillations and the resulting TDNS energy transport processes. Therefore, the energy flux paths are different from the typical Lissajous shapes. The relationships between the temperature bias and the energy flux that give rise to hysteresis are only possible

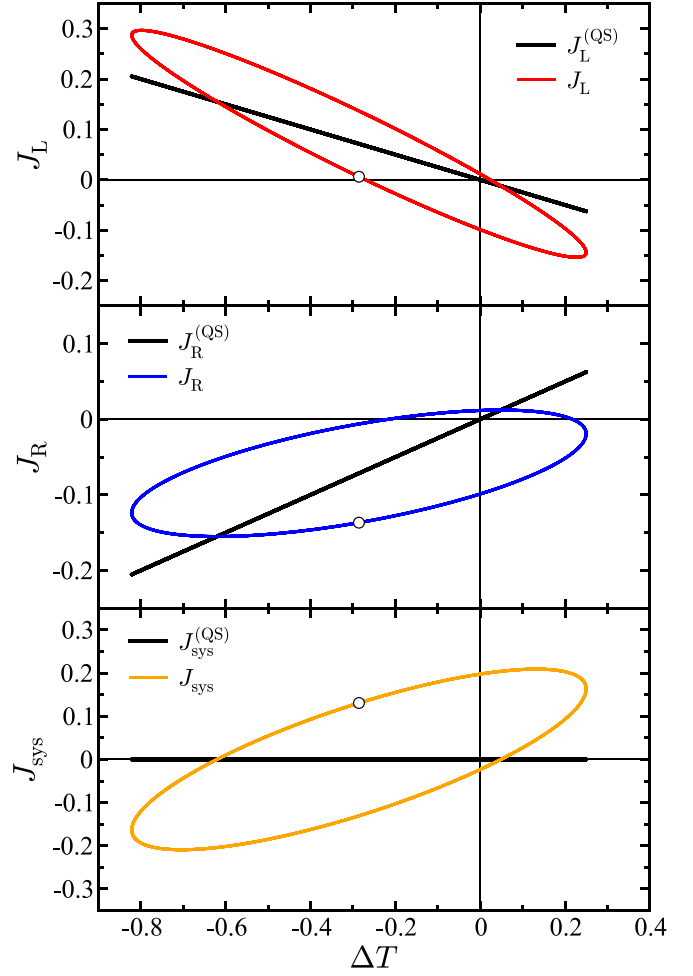


FIG. 4. Energy flux as a function of temperature difference for the left bath (top), right bath (middle), and the system (bottom) which is a free particle. The parameters are the same as Fig. 2. Each energy flux is shown in units of  $\gamma k_B T$  and the temperature difference  $\Delta T$  is shown in units of  $T$ . In each panel, the colored curve is the exact analytical result and the solid black line is the result given by the quasistatic expression. The marker on each curve marks the value of the respective energy flux at  $t = 0$ .

when the temperature oscillations are fast relative to the system relaxation rates and so the system is not in a quasistatic state.

As described by the equations in Sec. III, the energy fluxes will accumulate and dissipate over a certain period of time. The magnitude of energy storage and energy release are insightful to calculate, as they relate how much total energy is being stored and released by the system. This is analogous to electric charges accumulating in electric circuits. In Fig. 6 the energy obtained by the system over a period of oscillation is shown as a function of variation of the left system-bath coupling  $\gamma_L$  while holding the right coupling  $\gamma_R$  constant. The red line is the energy obtained by the system during one period of temperature oscillation and the blue line is energy released from the system during the same period. As the coupling strength to the left bath is increased, the energy obtained increases monotonically. The energy obtained and the energy released have equal magnitude but opposite signs.

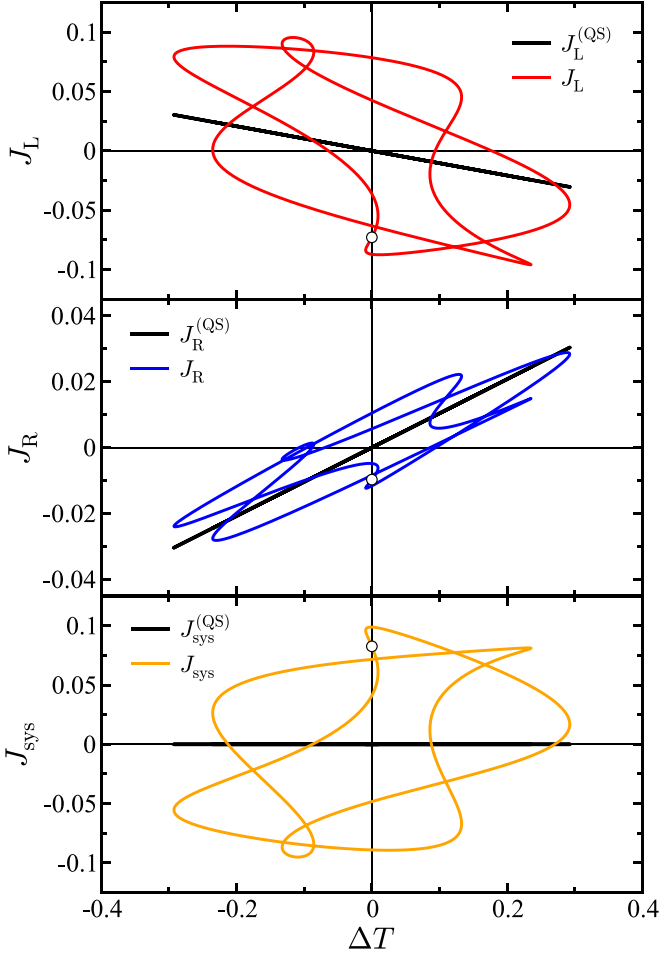


FIG. 5. Energy flux as a function of temperature difference for the left bath (top), right bath (middle), and the system (bottom) which is a free particle. The parameters are the same as Fig. 3. Each energy flux is shown in units of  $\gamma k_B T$  and the temperature difference  $\Delta T$  is shown in units of  $T$ . In each panel, the colored curve is the exact analytical result and the solid black line is the result given by the quasistatic expression. The marker on each curve marks the value of the respective energy flux at  $t = 0$ .

This illustrates that over a period of oscillation there is no net energy storage in the system. More complicated patterns and trends arise when extra layers of complexity are added, e.g., when nonzero potential energy forms are used as described in the next section (see also Fig. 9).

### B. Harmonic potential

Next, we examine the case in which the particle connecting the two heat baths moves in a harmonic potential. The equation of motion for a particle in the potential  $U(x) = \frac{1}{2}mkx^2$  can be written as

$$\begin{aligned} \dot{x} &= v, \\ \dot{v} &= -\gamma\dot{x} - kx + \xi_L(t) + \xi_R(t), \end{aligned} \quad (29)$$

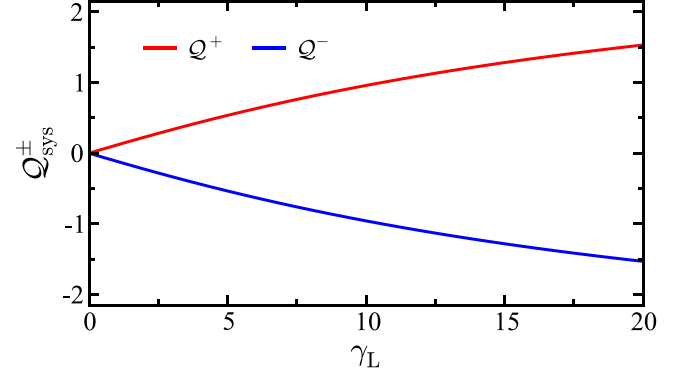


FIG. 6. Energy obtained (red top curve) and released (blue bottom curve) by the system over one period of temperature oscillation as function of the coupling parameter  $\gamma_L$  with  $\gamma_R = 2$  held constant. All other parameters are the same as Fig. 2. Energy is shown in units of  $k_B T$ . The coupling parameter is shown in units of  $1/T$ .

with  $\gamma = \gamma_L + \gamma_R$  as before. For convenience we write Eq. (29) as

$$\begin{pmatrix} \dot{x}(t) \\ \dot{v}(t) \end{pmatrix} = \begin{pmatrix} 0 & 1 \\ -k & -\gamma \end{pmatrix} \begin{pmatrix} x(t) \\ v(t) \end{pmatrix} + \begin{pmatrix} 0 \\ \xi_L(t) + \xi_R(t) \end{pmatrix}. \quad (30)$$

The complementary equation of Eq. (30) is

$$\begin{pmatrix} \dot{x}_c(t) \\ \dot{v}_c(t) \end{pmatrix} = \mathbf{A} \begin{pmatrix} x(t) \\ v(t) \end{pmatrix}, \quad (31)$$

with

$$\mathbf{A} = \begin{pmatrix} 0 & 1 \\ -k & -\gamma \end{pmatrix}. \quad (32)$$

Eigenvalues of  $\mathbf{A}$  are

$$\begin{aligned} \lambda_1 &= \frac{1}{2}(-\gamma - \sqrt{\gamma^2 - 4k}), \\ \lambda_2 &= \frac{1}{2}(-\gamma + \sqrt{\gamma^2 - 4k}). \end{aligned} \quad (33)$$

For simplicity, we define

$$\Delta\lambda = \lambda_2 - \lambda_1. \quad (34)$$

The fundamental matrix solution of Eq. (31) is

$$\mathbf{M}(t) = (\mathbf{v}_1 e^{\lambda_1 t} \quad \mathbf{v}_2 e^{\lambda_2 t}), \quad (35)$$

where  $\mathbf{v}_1$  and  $\mathbf{v}_2$  are eigenvectors. The solution of the initial value problem is

$$\begin{pmatrix} x_c(t) \\ v_c(t) \end{pmatrix} = \mathbf{M}(t)\mathbf{M}^{-1}(0) \begin{pmatrix} x_0 \\ v_0 \end{pmatrix}, \quad (36)$$

which can be expressed as

$$\begin{pmatrix} x_c(t) \\ v_c(t) \end{pmatrix} = \begin{pmatrix} \frac{e^{\lambda_1 t}(\lambda_2 x_0 - v_0) - e^{\lambda_2 t}(\lambda_1 x_0 - v_0)}{\Delta\lambda} \\ \frac{\lambda_1 e^{\lambda_1 t}(\lambda_2 x_0 - v_0) - \lambda_2 e^{\lambda_2 t}(\lambda_1 x_0 - v_0)}{\Delta\lambda} \end{pmatrix}. \quad (37)$$

The critical damping  $\lambda_1 = \lambda_2$  solution is obtained by taking the  $\lambda_1 \rightarrow \lambda_2$  limit in the previous equations.

The formal solution of the stochastic equation of motion (30) is

$$\begin{pmatrix} x(t) \\ v(t) \end{pmatrix} = \mathbf{M}(t)\mathbf{M}^{-1}(0)\begin{pmatrix} x_0 \\ v_0 \end{pmatrix} + \int_0^t \mathbf{M}(t)\mathbf{M}^{-1}(s) \begin{pmatrix} 0 \\ \xi_{\text{L}}(s) + \xi_{\text{R}}(s) \end{pmatrix} ds, \quad (38)$$

where the first term on the right-hand side is the complementary part of the solution. The formal solution can be written as

$$\begin{aligned} x(t) &= \frac{e^{\lambda_1 t}(\lambda_2 x_0 - v_0) - e^{\lambda_2 t}(\lambda_1 x_0 - v_0)}{\Delta\lambda} - \frac{1}{\Delta\lambda} \left( \int_0^t e^{\lambda_1(t-s)} \xi_{\text{L}}(s) ds + \int_0^t e^{\lambda_1(t-s)} \xi_{\text{R}}(s) ds \right) \\ &\quad + \frac{1}{\Delta\lambda} \left( \int_0^t e^{\lambda_2(t-s)} \xi_{\text{L}}(s) ds + \int_0^t e^{\lambda_2(t-s)} \xi_{\text{R}}(s) ds \right), \end{aligned} \quad (39)$$

$$\begin{aligned} v(t) &= \frac{\lambda_1 e^{\lambda_1 t}(\lambda_2 x_0 - v_0) - \lambda_2 e^{\lambda_2 t}(\lambda_1 x_0 - v_0)}{\Delta\lambda} - \frac{\lambda_1}{\Delta\lambda} \left( \int_0^t e^{\lambda_1(t-s)} \xi_{\text{L}}(s) ds + \int_0^t e^{\lambda_1(t-s)} \xi_{\text{R}}(s) ds \right) \\ &\quad + \frac{\lambda_2}{\Delta\lambda} \left( \int_0^t e^{\lambda_2(t-s)} \xi_{\text{L}}(s) ds + \int_0^t e^{\lambda_2(t-s)} \xi_{\text{R}}(s) ds \right). \end{aligned} \quad (40)$$

Using the formal solutions (39) and (40) and the noise correlations in Eq. (2), the noise-velocity correlation functions  $\langle \xi_{\text{L}}(t)v(t) \rangle$  and  $\langle \xi_{\text{R}}(t)v(t) \rangle$  in the heat current expressions in Eqs. (6) and (7) can be written as

$$\begin{aligned} \langle \xi_{\text{L}}(t)v(t) \rangle &= \langle \xi_{\text{L}}(t)v_c(t) \rangle - \frac{\lambda_1}{\Delta\lambda} \left( \int_0^t e^{\lambda_1(t-s)} \langle \xi_{\text{L}}(t)\xi_{\text{L}}(s) \rangle ds + \int_0^t e^{\lambda_1(t-s)} \langle \xi_{\text{L}}(t)\xi_{\text{R}}(s) \rangle ds \right) \\ &\quad + \frac{\lambda_2}{\Delta\lambda} \left( \int_0^t e^{\lambda_2(t-s)} \langle \xi_{\text{L}}(t)\xi_{\text{L}}(s) \rangle ds + \int_0^t e^{\lambda_2(t-s)} \langle \xi_{\text{L}}(t)\xi_{\text{R}}(s) \rangle ds \right) \\ &= \frac{\gamma_{\text{L}} k_{\text{B}} T_{\text{L}}(t)}{m}, \end{aligned} \quad (41)$$

$$\begin{aligned} \langle \xi_{\text{R}}(t)v(t) \rangle &= \langle \xi_{\text{R}}(t)v_c(t) \rangle - \frac{\lambda_1}{\Delta\lambda} \left( \int_0^t e^{\lambda_1(t-s)} \langle \xi_{\text{R}}(t)\xi_{\text{L}}(s) \rangle ds + \int_0^t e^{\lambda_1(t-s)} \langle \xi_{\text{R}}(t)\xi_{\text{R}}(s) \rangle ds \right) \\ &\quad + \frac{\lambda_2}{\Delta\lambda} \left( \int_0^t e^{\lambda_2(t-s)} \langle \xi_{\text{R}}(t)\xi_{\text{L}}(s) \rangle ds + \int_0^t e^{\lambda_2(t-s)} \langle \xi_{\text{R}}(t)\xi_{\text{R}}(s) \rangle ds \right) \\ &= \frac{\gamma_{\text{R}} k_{\text{B}} T_{\text{R}}(t)}{m}, \end{aligned} \quad (42)$$

here we have utilized  $\langle \xi_{\text{R}}(t)v_c(t) \rangle = \langle \xi_{\text{L}}(t)v_c(t) \rangle = 0$  from causality by noting that all terms in  $v_c(t)$  contain initial velocity  $v_0$  or initial position  $x_0$ .

The expectation value for the energy of the system is

$$\langle E(t) \rangle = \frac{1}{2} m \langle v^2(t) \rangle + \frac{1}{2} m k \langle x^2(t) \rangle. \quad (43)$$

The second velocity moment  $\langle v^2(t) \rangle$  can be evaluated by squaring the formal solution Eq. (40) and applying the noise correlations leading to

$$\begin{aligned} \langle v^2(t) \rangle &= v_c^2(t) + \left( \frac{1}{\Delta\lambda} \right)^2 \left( \lambda_1^2 \int_0^t \int_0^t e^{\lambda_1(2t-s_1-s_2)} \langle \xi_{\text{L}}(s_1)\xi_{\text{L}}(s_2) \rangle ds_1 ds_2 + \lambda_1^2 \int_0^t \int_0^t e^{\lambda_1(2t-s_1-s_2)} \langle \xi_{\text{R}}(s_1)\xi_{\text{R}}(s_2) \rangle ds_1 ds_2 \right. \\ &\quad + \lambda_2^2 \int_0^t \int_0^t e^{\lambda_2(2t-s_1-s_2)} \langle \xi_{\text{L}}(s_1)\xi_{\text{L}}(s_2) \rangle ds_1 ds_2 + \lambda_2^2 \int_0^t \int_0^t e^{\lambda_2(2t-s_1-s_2)} \langle \xi_{\text{R}}(s_1)\xi_{\text{R}}(s_2) \rangle ds_1 ds_2 \\ &\quad \left. - 2k \int_0^t \int_0^t e^{\lambda_1(t-s_1)+\lambda_2(t-s_2)} \langle \xi_{\text{L}}(s_1)\xi_{\text{L}}(s_2) \rangle ds_1 ds_2 - 2k \int_0^t \int_0^t e^{\lambda_1(t-s_1)+\lambda_2(t-s_2)} \langle \xi_{\text{R}}(s_1)\xi_{\text{R}}(s_2) \rangle ds_1 ds_2 \right) \\ &= v_c^2(t) - \left( \frac{1}{\Delta\lambda} \right)^2 \left( \frac{\gamma k_{\text{B}} T}{m} \left( \lambda_1(1 - e^{2\lambda_1 t}) + \lambda_2(1 - e^{2\lambda_2 t}) + \frac{4k(1 - e^{-\gamma t})}{\gamma} \right) \right. \\ &\quad \left. + \frac{2k_{\text{B}} \lambda_1^2}{m} \left( \frac{\gamma_{\text{L}} \Delta T_{\text{L}} (2\lambda_1 \sin(\omega_{\text{L}} t) + \omega_{\text{L}} \cos(\omega_{\text{L}} t) - \omega_{\text{L}} e^{2\lambda_1 t})}{4\lambda_1^2 + \omega_{\text{L}}^2} + \frac{\gamma_{\text{R}} \Delta T_{\text{R}} (2\lambda_1 \sin(\omega_{\text{R}} t) + \omega_{\text{R}} \cos(\omega_{\text{R}} t) - \omega_{\text{R}} e^{2\lambda_1 t})}{4\lambda_1^2 + \omega_{\text{R}}^2} \right) \right) \end{aligned}$$



$$+ \frac{2k_B\lambda_2^2}{m} \left( \frac{\gamma_L \Delta T_L (2\lambda_2 \sin(\omega_L t) + \omega_L \cos(\omega_L t) - \omega_L e^{2\lambda_2 t})}{4\lambda_2^2 + \omega_L^2} + \frac{\gamma_R \Delta T_R (2\lambda_2 \sin(\omega_R t) + \omega_R \cos(\omega_R t) - \omega_R e^{2\lambda_2 t})}{4\lambda_2^2 + \omega_R^2} \right) - k \frac{4k_B}{m} \left( \frac{\gamma_L \Delta T_L (\omega_L \cos(\omega_L t) - \gamma \sin(\omega_L t) - \omega_L e^{-\gamma t})}{\gamma^2 + \omega_L^2} + \frac{\gamma_R \Delta T_R (\omega_R \cos(\omega_R t) - \gamma \sin(\omega_R t) - \omega_R e^{-\gamma t})}{\gamma^2 + \omega_R^2} \right), \quad (44)$$

where we have excluded the cross-correlation terms between the two baths (which all are equal zero) in the top equation for brevity. The  $\langle x^2(t) \rangle$  term in Eq. (43) is evaluated in a similar fashion to  $\langle v^2(t) \rangle$ , leading to

$$\begin{aligned} \langle x^2(t) \rangle = & x_c^2(t) - \left( \frac{1}{\Delta\lambda} \right)^2 \left( \frac{\gamma k_B T}{m} \left[ \left( \frac{1 - e^{2\lambda_1 t}}{\lambda_1} \right) + \left( \frac{1 - e^{2\lambda_2 t}}{\lambda_2} \right) + 4 \left( \frac{1 - e^{-\gamma t}}{\gamma} \right) \right] \right. \\ & + \frac{2k_B}{m} \left\{ \frac{\gamma_L \Delta T_L [2\lambda_1 \sin(\omega_L t) + \omega_L \cos(\omega_L t) - \omega_L e^{2\lambda_1 t}]}{4\lambda_1^2 + \omega_L^2} + \frac{\gamma_R \Delta T_R [2\lambda_1 \sin(\omega_R t) + \omega_R \cos(\omega_R t) - \omega_R e^{2\lambda_1 t}]}{4\lambda_1^2 + \omega_R^2} \right\} \\ & + \frac{2k_B}{m} \left\{ \frac{\gamma_L \Delta T_L [2\lambda_2 \sin(\omega_L t) + \omega_L \cos(\omega_L t) - \omega_L e^{2\lambda_2 t}]}{4\lambda_2^2 + \omega_L^2} + \frac{\gamma_R \Delta T_R [2\lambda_2 \sin(\omega_R t) + \omega_R \cos(\omega_R t) - \omega_R e^{2\lambda_2 t}]}{4\lambda_2^2 + \omega_R^2} \right\} \\ & \left. - \frac{4k_B}{m} \left\{ \frac{\gamma_L \Delta T_L [\omega_L \cos(\omega_L t) - \gamma \sin(\omega_L t) - \omega_L e^{-\gamma t}]}{\gamma^2 + \omega_L^2} + \frac{\gamma_R \Delta T_R [\omega_R \cos(\omega_R t) - \gamma \sin(\omega_R t) - \omega_R e^{-\gamma t}]}{\gamma^2 + \omega_R^2} \right\} \right). \quad (45) \end{aligned}$$

The energy flux expressions are obtained by substituting the correlation functions derived in this subsection into Eqs. (6)–(8). We are mostly concerned with the long-time limit of these expressions in which the system approaches a TDNS. The energy flux expressions in the TDNS are

$$\begin{aligned} J_L(t) = & -\gamma_L k_B T_L(t) - \gamma_L \left( \frac{1}{\Delta\lambda} \right)^2 \left( k_B T (4k - \gamma^2) \right. \\ & + 2k_B \lambda_1^2 \left\{ \frac{\gamma_L \Delta T_L [2\lambda_1 \sin(\omega_L t) + \omega_L \cos(\omega_L t)]}{4\lambda_1^2 + \omega_L^2} + \frac{\gamma_R \Delta T_R [2\lambda_1 \sin(\omega_R t) + \omega_R \cos(\omega_R t)]}{4\lambda_1^2 + \omega_R^2} \right\} \\ & + 2k_B \lambda_2^2 \left\{ \frac{\gamma_L \Delta T_L [2\lambda_2 \sin(\omega_L t) + \omega_L \cos(\omega_L t)]}{4\lambda_2^2 + \omega_L^2} + \frac{\gamma_R \Delta T_R [2\lambda_2 \sin(\omega_R t) + \omega_R \cos(\omega_R t)]}{4\lambda_2^2 + \omega_R^2} \right\} \\ & \left. - 4\lambda_1 \lambda_2 k_B \left\{ \frac{\gamma_L \Delta T_L [\omega_L \cos(\omega_L t) - \gamma \sin(\omega_L t)]}{\gamma^2 + \omega_L^2} + \frac{\gamma_R \Delta T_R [\omega_R \cos(\omega_R t) - \gamma \sin(\omega_R t)]}{\gamma^2 + \omega_R^2} \right\} \right), \quad (46) \end{aligned}$$

$$\begin{aligned} J_R(t) = & -\gamma_R k_B T_R(t) - \gamma_R \left( \frac{1}{\Delta\lambda} \right)^2 \left( k_B T (4k - \gamma^2) \right. \\ & + 2k_B \lambda_1^2 \left\{ \frac{\gamma_L \Delta T_L [2\lambda_1 \sin(\omega_L t) + \omega_L \cos(\omega_L t)]}{4\lambda_1^2 + \omega_L^2} + \frac{\gamma_R \Delta T_R [2\lambda_1 \sin(\omega_R t) + \omega_R \cos(\omega_R t)]}{4\lambda_1^2 + \omega_R^2} \right\} \\ & + 2k_B \lambda_2^2 \left\{ \frac{\gamma_L \Delta T_L [2\lambda_2 \sin(\omega_L t) + \omega_L \cos(\omega_L t)]}{4\lambda_2^2 + \omega_L^2} + \frac{\gamma_R \Delta T_R [2\lambda_2 \sin(\omega_R t) + \omega_R \cos(\omega_R t)]}{4\lambda_2^2 + \omega_R^2} \right\} \\ & \left. - 4\lambda_1 \lambda_2 k_B \left\{ \frac{\gamma_L \Delta T_L [\omega_L \cos(\omega_L t) - \gamma \sin(\omega_L t)]}{\gamma^2 + \omega_L^2} + \frac{\gamma_R \Delta T_R [\omega_R \cos(\omega_R t) - \gamma \sin(\omega_R t)]}{\gamma^2 + \omega_R^2} \right\} \right), \quad (47) \end{aligned}$$

$$\begin{aligned} J_{\text{sys}}(t) = & \left( \frac{1}{\Delta\lambda} \right)^2 \left( k_B (\lambda_1^2 + k) \left\{ \frac{\gamma_L \Delta T_L \omega_L [\omega_L \sin(\omega_L t) - 2\lambda_1 \cos(\omega_L t)]}{4\lambda_1^2 + \omega_L^2} + \frac{\gamma_R \Delta T_R \omega_R [\omega_R \sin(\omega_R t) - 2\lambda_1 \cos(\omega_R t)]}{4\lambda_1^2 + \omega_R^2} \right\} \right. \\ & + k_B (\lambda_2^2 + k) \left\{ \frac{\gamma_L \Delta T_L \omega_L [\omega_L \sin(\omega_L t) - 2\lambda_2 \cos(\omega_L t)]}{4\lambda_2^2 + \omega_L^2} + \frac{\gamma_R \Delta T_R \omega_R [\omega_R \sin(\omega_R t) - 2\lambda_2 \cos(\omega_R t)]}{4\lambda_2^2 + \omega_R^2} \right\} \\ & \left. - 4\lambda_1 \lambda_2 k_B \left\{ \frac{\gamma_L \Delta T_L \omega_L [\gamma \cos(\omega_L t) + \omega_L \sin(\omega_L t)]}{\gamma^2 + \omega_L^2} + \frac{\gamma_R \Delta T_R \omega_R [\gamma \cos(\omega_R t) + \omega_R \sin(\omega_R t)]}{\gamma^2 + \omega_R^2} \right\} \right). \quad (48) \end{aligned}$$

Two observations are of note:

(1) Evaluating the net energy change over a period of temperature driving using Eq. (10), contributions from the trigonometric functions are zero. Therefore, for a single particle (a free particle or a particle in a harmonic potential) connecting two heat baths, the periodic temperature driving

does not lead to enhanced energy transport in comparison to static temperature limit.

(2) Due to the temperature oscillations, the energy fluxes depend on  $k$ . This differs from the single-particle case without temperature driving in which the energy fluxes are independent of  $k$  [13].

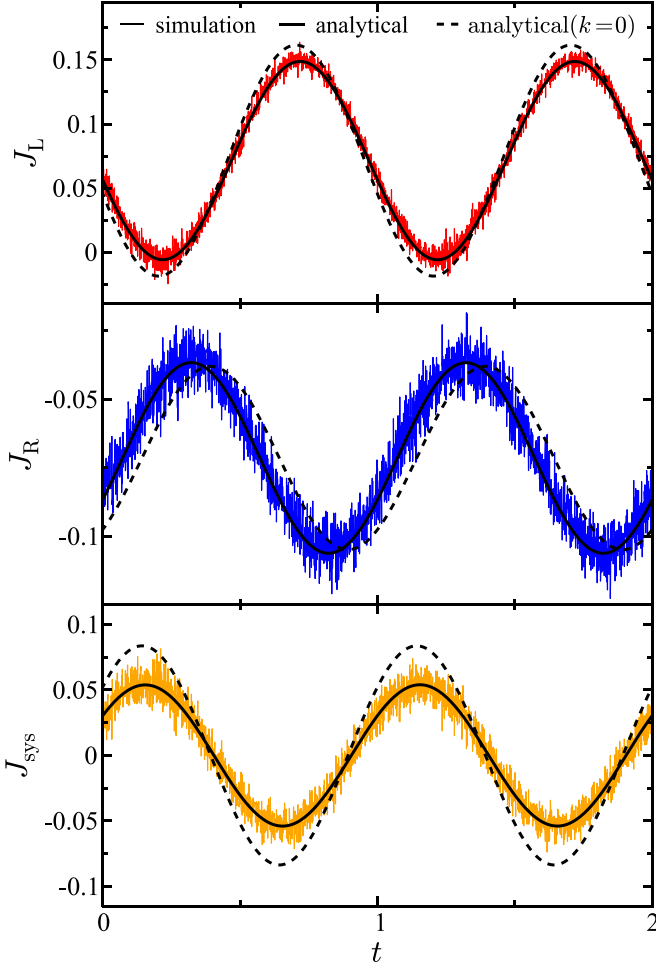


FIG. 7. Time-dependence of the energy fluxes in the case of a particle in a harmonic potential connecting two heat baths with oscillating temperatures. Each energy flux is shown in units of  $\gamma k_B T$ . Time is shown in units of the total oscillation period  $\mathcal{T}$ . Parameters are  $k = 5$ ,  $\gamma = 2$  ( $\gamma_L = 1$ ,  $\gamma_R = 1$ ),  $m = 1$ ,  $T_L^{(0)} = 0.8$ ,  $T_R^{(0)} = 1.07$ ,  $\Delta T_L = 0.2$ ,  $\Delta T_R = 0$ ,  $\omega_L = 5$ ,  $\omega_R = 0$ . In each panel, the solid black curve is the exact analytical result, the dashed black curve is the analytical result in the free particle  $k = 0$  limit, and the noisy colored curves are the results generated from molecular dynamics simulations.

In the quasistatic ( $\omega_L/\gamma$ ,  $\omega_R/\gamma$ )  $\rightarrow$  (0, 0) limit, the derived analytical expressions reduce to the same energy flux expressions that were obtained for a free particle:

$$J_L^{(QS)}(t) = k_B \frac{\gamma_L \gamma_R}{\gamma_L + \gamma_R} [T_R(t) - T_L(t)], \quad (49)$$

$$J_R^{(QS)}(t) = k_B \frac{\gamma_L \gamma_R}{\gamma_L + \gamma_R} [T_L(t) - T_R(t)], \quad (50)$$

$$J_{\text{sys}}^{(QS)}(t) = 0. \quad (51)$$

This implies that in the QS limit, the energy flux is independent of the potential form for a harmonic system. In the static limit defined by  $(\Delta T_L, \Delta T_R) \rightarrow (0, 0)$ , the system again reduces to the well-known form for the heat current of a single particle connecting two heat baths:

$$J_L^{(S)} = k_B \frac{\gamma_L \gamma_R}{\gamma_L + \gamma_R} (T_R^{(0)} - T_L^{(0)}), \quad (52)$$

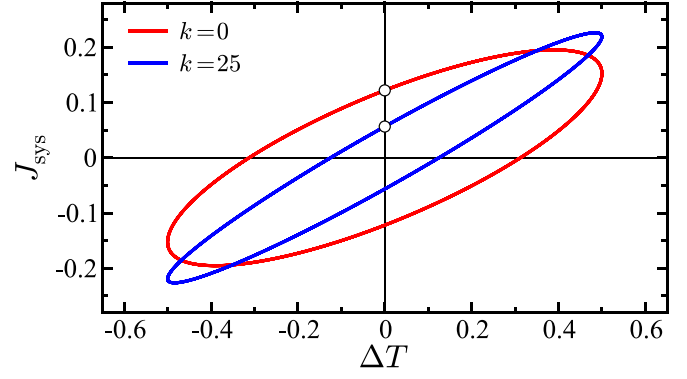


FIG. 8. System energy flux as a function of temperature difference for a particle in a harmonic potential. Hysteresis loops are shown for  $k = 0$  (red wider loop) and  $k = 25$  (blue more narrow loop). The temperatures of the baths are  $T_R^{(0)} = T_L^{(0)} = 1$ . Other parameters are the same as Fig. 2. Each energy flux is shown in units of  $\gamma k_B T$  and the temperature difference  $\Delta T$  is shown in units of  $T$ . The marker on each curve marks the value of the respective energy flux at  $t = 0$ .

$$J_R^{(S)} = k_B \frac{\gamma_L \gamma_R}{\gamma_L + \gamma_R} (T_L^{(0)} - T_R^{(0)}), \quad (53)$$

$$J_{\text{sys}}^{(S)} = 0, \quad (54)$$

which are independent of the potential form, as shown by Lebowitz [13].

Figure 7 shows the time-dependent energy fluxes for the left bath, right bath, and the system—in this case a particle moving in a harmonic potential. As in the free-particle case, the MD simulation results are in excellent agreement with the analytical results. The dashed lines, representing the results for a free particle, deviate from the results for a harmonic potential. The difference between free particle and the harmonic particle are observed as changes in the energy flux oscillation phase and/or changes to the magnitude of oscillation. For example, in the system energy flux, increasing  $k$  away from the free particle  $k = 0$  limit results in a reduced oscillation amplitude.

The shape of the energy flux hysteresis loops are affected by the harmonic forces in the particle potential. Figure 8 shows hysteresis loops for two values of  $k$  in the case where one bath temperature is oscillating and the other is constant (the parameters are the same as in Fig. 4). The characteristic shape of the loops are similar to the free-particle case with the noticeable difference that the added external potential makes the hysteresis loop narrower, a reflection of the reduced energy flux oscillation amplitude.

The energy obtained by the system  $Q_{\text{sys}}^+$  over a period of oscillation is shown in Fig. 9 as a function of the parameter  $k$ . Results are shown for the parameters used in Fig. 2 (solid curve) and in Fig. 3 (dashed curve). In both cases, the energy obtained by the system goes down first with increasing  $k$ , then goes up approaching a horizontal asymptotic limit. The minima observed with respect to variation of  $k$  values are interesting features of the system. No first-order parametric resonances are observed that correspond to the minima in the  $Q_{\text{sys}}^+$  versus  $k$  curves, meaning that the minima do not

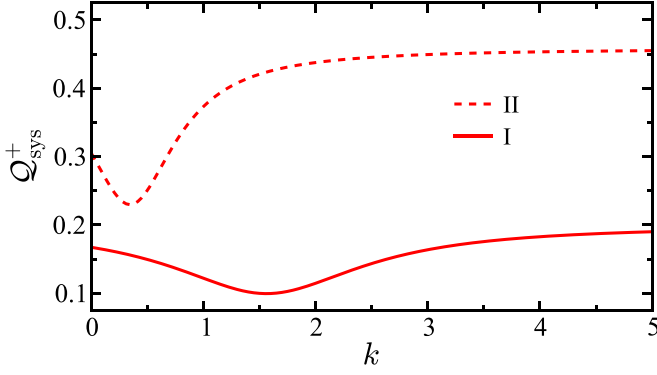


FIG. 9. Energy obtained by the system over one period of oscillation as function of  $k$  for two sets of parameters denoted I and II. Parameter set I, shown as a solid curve, are the same as in Fig. 2. Parameter set II, shown as a dashed curve, are the same as in Fig. 3. Energy is shown in units of  $k_B T$  and  $k$  is shown in units of  $\gamma^2$ .

correspond to  $k$  values equal to  $\omega_L^2$ ,  $\omega_R^2$ ,  $\gamma_L^2$ , or  $\gamma_R^2$ . Changing the friction parameters  $\gamma_L$  and/or  $\gamma_R$  alters the shape of the  $Q_{\text{sys}}^+$  versus  $k$  curve, but does not alter the location of the minimum. However, the location of the minimum is dependent on the temperature oscillation frequencies. Generally, as the temperature oscillation frequencies are increased, the location of the minimum corresponds to a larger value of  $k$ . Possible higher-order resonance and off-resonance states may give rise to the dip in  $Q_{\text{sys}}^+$  with respect to variation of  $k$ . The overall trends of the two parameter sets shown in Fig. 9 are similar, but the case with two baths oscillating with different frequencies results in more energy being obtained by the system across the entire range of  $k$ . We conjecture this is due to constructive interference effects.

## V. CONCLUSIONS

The energy transport properties of a particle connecting two heat baths with different temperatures where the temperature difference between baths is oscillating in time have been derived. A stochastic Langevin formalism has been applied to describe the energy transport in different regimes of fast/slow temperature oscillations and system-bath coupling strengths. Analytical expressions have been derived for the time-dependent energy flux of each heat bath and for the

system itself for two cases: (a) a free particle and (b) a particle in a harmonic potential. We find that the instantaneous energy fluxes (the heat currents) are time-dependent, as expected, due to the temperature oscillations and that in the long-time limit the system relaxes to a time-dependent nonequilibrium state. Energy exchange between the system and the heat baths can be significantly affected by multiple factors such as the temperature oscillation frequency, the magnitude of the temperature oscillation, and, in the case that the temperatures of both baths are oscillating, the ratio between the two oscillation frequencies. In the limit of fast temperature oscillation relative to the relaxation rate of the system, significant differences are observed in the energy fluxes in comparison to the results obtained in the quasistatic limit defined by slow temperature oscillations.

The presented results illustrate that dynamical and inertial effects in the energy flux induced by fast temperature oscillations can give rise to complex energy transport hysteresis effects. Our findings also suggest that applying time-periodic temperature modulations could be a possible pathway to control energy flow in molecular devices and nanoscale systems. The application of these effects in the design of thermal devices with memory is a potential future research direction. In the case of a single particle, either a free particle or a particle in a harmonic potential, the thermal conductivity is not enhanced by the temperature oscillations in comparison to keeping the temperature gradient static. An increase in thermal conductivity due to temperature oscillations, which has been observed in macroscale systems, may arise at the molecular level due to anharmonicities in the system or interactions between multiples particles—both of which are not included in the present model but are targets for future work.

## ACKNOWLEDGMENTS

We acknowledge support from the Los Alamos National Laboratory (LANL) Directed Research and Development funds (LDRD). This research was performed in part at the Center for Nonlinear Studies (CNLS) at LANL. The computing resources used to perform this research were provided by the LANL Institutional Computing Program.

## APPENDIX: FIGURE PARAMETERS

The parameter values used in the figures are listed in Table I.

TABLE I. Parameter values used in each listed figure. All values are given in reduced units with characteristic dimensions:  $\tilde{\sigma} = 1 \text{ \AA}$ ,  $\tilde{\tau} = 1 \text{ ps}$ ,  $\tilde{m} = 10 m_u$ , and  $\tilde{T} = 300 \text{ K}$ .

Figure	$m$	$\gamma_L$	$\gamma_R$	$\gamma$	$\omega_L$	$\omega_R$	$\Delta T_L$	$\Delta T_R$	$T_L^{(0)}$	$T_R^{(0)}$	$k$
2	1	1	1	2	5	0	0.5	0	0.8	1.07	0
3	1	1.5	0.2	1.7	2	5	0.2	0.1	1	1	0
4	1	1	1	2	5	0	0.5	0	0.8	1.07	0
5	1	1.5	0.2	1.7	2	5	0.2	0.1	1	1	0
6	1	–	2	–	5	0	0.5	0	0.8	1.07	0
7	1	1	1	2	5	0	0.2	0	0.8	1.07	5
8	1	1	1	2	5	0	0.5	0	1	1	25

- [1] D. G. Cahill, K. Goodson, and A. Majumdar, *J. Heat Transfer* **124**, 223 (2002).
- [2] D. G. Cahill, W. K. Ford, K. E. Goodson, G. D. Mahan, A. Majumdar, H. J. Maris, R. Merlin, and S. R. Phillpot, *J. Appl. Phys.* **93**, 793 (2003).
- [3] A. Dhar, *Adv. Phys.* **57**, 457 (2008).
- [4] Y. Dubi and M. Di Ventra, *Rev. Mod. Phys.* **83**, 131 (2011).
- [5] S. Narayana and Y. Sato, *Phys. Rev. Lett.* **108**, 214303 (2012).
- [6] M. Maldovan, *Nature* **503**, 209 (2013).
- [7] D. Segal and B. K. Agarwalla, *Annu. Rev. Phys. Chem.* **67**, 185 (2016).
- [8] H. Ness, A. Genina, L. Stella, C. D. Lorenz, and L. Kantorovich, *Phys. Rev. B* **93**, 174303 (2016).
- [9] H. Ness, L. Stella, C. D. Lorenz, and L. Kantorovich, *J. Chem. Phys.* **146**, 164103 (2017).
- [10] E. S. Nascimento and W. A. M. Morgado, *J. Phys. A: Math. Theor.* **55**, 395003 (2022).
- [11] N. Li, J. Ren, L. Wang, G. Zhang, P. Hänggi, and B. Li, *Rev. Mod. Phys.* **84**, 1045 (2012).
- [12] S. Sabhapandit, *Phys. Rev. E* **85**, 021108 (2012).
- [13] J. L. Lebowitz, *Phys. Rev.* **114**, 1192 (1959).
- [14] Z. Rieder, J. L. Lebowitz, and E. Lieb, *J. Math. Phys.* **8**, 1073 (1967).
- [15] A. Casher and J. L. Lebowitz, *J. Math. Phys.* **12**, 1701 (1971).
- [16] A. Dhar and J. L. Lebowitz, *Phys. Rev. Lett.* **100**, 134301 (2008).
- [17] V. Kannan, A. Dhar, and J. L. Lebowitz, *Phys. Rev. E* **85**, 041118 (2012).
- [18] D. Segal, A. Nitzan, and P. Hänggi, *J. Chem. Phys.* **119**, 6840 (2003).
- [19] D. Segal and A. Nitzan, *Phys. Rev. Lett.* **94**, 034301 (2005).
- [20] A. Dhar and R. Dandekar, *Physica A* **418**, 49 (2015).
- [21] K. A. Velizhanin, S. Sahu, C.-C. Chien, Y. Dubi, and M. Zwolak, *Sci. Rep.* **5**, 17506 (2015).
- [22] Y. Murashita and M. Esposito, *Phys. Rev. E* **94**, 062148 (2016).
- [23] G. T. Craven and A. Nitzan, *Proc. Natl. Acad. Sci. USA* **113**, 9421 (2016).
- [24] D. V. Matyushov, *Proc. Natl. Acad. Sci. USA* **113**, 9401 (2016).
- [25] G. T. Craven and A. Nitzan, *J. Chem. Phys.* **146**, 092305 (2017).
- [26] G. T. Craven and A. Nitzan, *Phys. Rev. Lett.* **118**, 207201 (2017).
- [27] R. Chen, G. T. Craven, and A. Nitzan, *J. Chem. Phys.* **147**, 124101 (2017).
- [28] G. T. Craven and A. Nitzan, *Nano Lett.* **20**, 989 (2020).
- [29] M. A. Ochoa, *Phys. Rev. E* **106**, 064113 (2022).
- [30] D. M. Leitner, *Annu. Rev. Phys. Chem.* **59**, 233 (2008).
- [31] M. Galperin, A. Nitzan, and M. A. Ratner, *Phys. Rev. B* **75**, 155312 (2007).
- [32] M. A. Ratner, *Nat. Nanotechnol.* **8**, 378 (2013).
- [33] J. S. Lim, R. López, and D. Sánchez, *Phys. Rev. B* **88**, 201304(R) (2013).
- [34] M. Esposito, M. A. Ochoa, and M. Galperin, *Phys. Rev. B* **91**, 115417 (2015).
- [35] B. Russ, A. Glaudell, J. J. Urban, M. L. Chabiny, and R. A. Segalman, *Nat. Rev. Mater.* **1**, 16050 (2016).
- [36] L. Cui, R. Miao, C. Jiang, E. Meyhofer, and P. Reddy, *J. Chem. Phys.* **146**, 092201 (2017).
- [37] P. Gehring, J. K. Sowa, C. Hsu, J. de Bruijckere, M. van der Star, J. J. Le Roy, L. Bogani, E. M. Gauger, and H. S. van der Zant, *Nat. Nanotechnol.* **16**, 426 (2021).
- [38] Q. Li, I. Duchemin, S. Xiong, G. C. Solomon, and D. Donadio, *J. Phys. Chem. C* **119**, 24636 (2015).
- [39] R. Chen, I. Sharony, and A. Nitzan, *J. Phys. Chem. Lett.* **11**, 4261 (2020).
- [40] I. Sharony, R. Chen, and A. Nitzan, *J. Chem. Phys.* **153**, 144113 (2020).
- [41] L. Cui, S. Hur, Z. A. Akbar, J. C. Klöckner, W. Jeong, F. Pauly, S.-Y. Jang, P. Reddy, and E. Meyhofer, *Nature* **572**, 628 (2019).
- [42] N. Mosso, H. Sadeghi, A. Gemma, S. Sangtarash, U. Drechsler, C. Lambert, and B. Gotsmann, *Nano Lett.* **19**, 7614 (2019).
- [43] G. T. Craven, T. Bartsch, and R. Hernandez, *J. Chem. Phys.* **142**, 074108 (2015).
- [44] G. T. Craven and R. Hernandez, *Phys. Rev. Lett.* **115**, 148301 (2015).
- [45] G. T. Craven, A. Junginger, and R. Hernandez, *Phys. Rev. E* **96**, 022222 (2017).
- [46] F. Revuelta, G. T. Craven, T. Bartsch, and R. Hernandez, *J. Chem. Phys.* **147**, 074104 (2017).
- [47] F. Bonetto, J. L. Lebowitz, and L. Rey-Bellet, *Mathematical Physics* (Imperial College, London, 2000), pp. 128–150.
- [48] F. Bonetto, J. L. Lebowitz, and J. Lukkarinen, *J. Stat. Phys.* **116**, 783 (2004).
- [49] D. Segal, *Phys. Rev. E* **79**, 012103 (2009).
- [50] C. W. Chang, D. Okawa, H. Garcia, A. Majumdar, and A. Zettl, *Phys. Rev. Lett.* **101**, 075903 (2008).
- [51] G. T. Craven and A. Nitzan, *J. Chem. Phys.* **158** (2023).
- [52] P. Urban, P. Hanzelka, T. Králik, V. Musilová, and L. Skrbek, *Phys. Rev. Lett.* **128**, 134502 (2022).
- [53] P. J. Goss and J. Peccoud, *Proc. Natl. Acad. Sci. USA* **95**, 6750 (1998).
- [54] M. Platkov and M. Gruebele, *J. Chem. Phys.* **141**, 07B616\_1 (2014).
- [55] J. Rosnagel, S. T. Dawkins, K. N. Tolazzi, O. Abah, E. Lutz, F. Schmidt-Kaler, and K. Singer, *Science* **352**, 325 (2016).
- [56] C. R. Bowen, J. Taylor, E. LeBoulbar, D. Zabeck, A. Chauhan, and R. Vaish, *Energy Environ. Sci.* **7**, 3836 (2014).
- [57] K. Yamamoto, A. Kawasaki, T. Chinen, and K. Ryugo, *Crystals* **11**, 880 (2021).
- [58] P. Lheritier, A. Torelló, T. Usui, Y. Nouchokgwe, A. Aravindhan, J. Li, U. Prah, V. Kovacova, O. Bouton, S. Hirose *et al.*, *Nature* **609**, 718 (2022).
- [59] I. Gur, K. Sawyer, and R. Prasher, *Science* **335**, 1454 (2012).
- [60] C.-Y. Wang, T. Liu, X.-G. Yang, S. Ge, N. V. Stanley, E. S. Rountree, Y. Leng, and B. D. McCarthy, *Nature* **611**, 485 (2022).
- [61] R. Bartussek, P. Hänggi, and J. G. Kissner, *Europhys. Lett.* **28**, 459 (1994).
- [62] F. Zhan, N. Li, S. Kohler, and P. Hänggi, *Phys. Rev. E* **80**, 061115 (2009).
- [63] Y. Zhang and J. Chen, *Physica A* **387**, 3443 (2008).
- [64] P. Ben-Abdallah, *AIP Adv.* **7**, 065002 (2017).
- [65] J. Ordonez-Miranda, Y. Ezzahri, J. A. Tiburcio-Moreno, K. Joulain, and J. Drevillon, *Phys. Rev. Lett.* **123**, 025901 (2019).
- [66] S. Sadat, Y. J. Chua, W. Lee, Y. Ganjeh, K. Kurabayashi, E. Meyhofer, and P. Reddy, *Appl. Phys. Lett.* **99**, 043106 (2011).
- [67] E. Shoifet, G. Schulz, and C. Schick, *Thermochim. Acta* **603**, 227 (2015).

- [68] P. Reimann, *Phys. Rep.* **361**, 57 (2002).
- [69] J. Brey and J. Casado, *J. Stat. Phys.* **61**, 713 (1990).
- [70] A. V. Popov and R. Hernandez, *J. Chem. Phys.* **126**, 244506 (2007).
- [71] A. V. Popov and R. Hernandez, *Phys. Rev. E* **88**, 032145 (2013).
- [72] I. J. Ford, Z. P. L. Laker, and H. J. Charlesworth, *Phys. Rev. E* **92**, 042108 (2015).
- [73] K. Brandner, K. Saito, and U. Seifert, *Phys. Rev. X* **5**, 031019 (2015).
- [74] K. Brandner and U. Seifert, *Phys. Rev. E* **93**, 062134 (2016).
- [75] S. Awasthi and S. B. Dutta, *Phys. Rev. E* **103**, 062143 (2021).
- [76] P. Portugal, F. Brange, and C. Flindt, *Phys. Rev. Res.* **4**, 043112 (2022).
- [77] J. Ordonez-Miranda, R. Anufriev, M. Nomura, and S. Volz, *Phys. Rev. B* **106**, L100102 (2022).
- [78] Y. Lanoiselée, A. Stanislavsky, D. Calebiro, and A. Weron, *Phys. Rev. E* **106**, 064127 (2022).
- [79] K. Sekimoto, *Prog. Theor. Phys. Suppl.* **130**, 17 (1998).
- [80] R. Fu, O. M. Miangolarra, A. Taghvaei, Y. Chen, and T. T. Georgiou, in *Proceedings of the 59th IEEE Conference on Decision and Control (CDC)* (IEEE, 2020), pp. 3034–3039.
- [81] F. Zamponi, F. Bonetto, L. F. Cugliandolo, and J. Kurchan, *J. Stat. Mech.* (2005) P09013.
- [82] G. T. Craven, R. Chen, and A. Nitzan, *J. Chem. Phys.* **149**, 104103 (2018).
- [83] G. T. Craven and A. Nitzan, *J. Chem. Phys.* **148**, 044101 (2018).
- [84] F. Caravelli and J. P. Carbajal, *Technologies* **6**, 118 (2018).
- [85] Y. van De Burgt, A. Melianas, S. T. Keene, G. Malliaras, and A. Salleo, *Nat. Electron.* **1**, 386 (2018).
- [86] V. K. Sangwan and M. C. Hersam, *Nat. Nanotechnol.* **15**, 517 (2020).
- [87] Y. V. Pershin and M. D. Ventra, *Adv. Phys.* **60**, 145 (2011).